RSC Advances

PAPER

View Article Online
View Journal | View Issue

Check for updates

Cite this: RSC Adv., 2023, 13, 16363

Selective hydrogenation of dimethyl terephthalate over a potassium-modified Ni/SiO_2 catalyst†

Han Xiao,‡[a] Chao Zhang,‡[a] Jiaojiao Zhao,[b] Zhaohui Zheng[c] and Yuehui Li*[b]

Received 4th April 2023
Accepted 22nd May 2023

DOI: 10.1039/d3ra02223d

rsc.li/rsc-advances

Selective hydrogenation of dimethyl terephthalate (DMT) is an ideal way to prepare 1,4-cyclohexane dicarboxylate (DMCD), an important intermediate and monomer. Even though noble metal-based catalysts (*e.g.*, Ru, Pd) have been developed for selective hydrogenation of DMT, the use of non-precious Ni catalysts to achieve high activity and selectivity is still challenging. In this study, we present that only 0.5 wt% of KF by post-impregnated doping can significantly improve the performance of Ni/SiO_2 catalysts (83% *vs.* 96% selectivity; 41% *vs.* 95% conversion). The selectivity of DMCD can be up to 97%, which is the highest reported over Ni catalysts. The boosting effect of KF modification might be due to higher amounts of Ni(0) species and lower amounts of moderate acidic sites, which are beneficial for selective hydrogenation of phenyl rings over hydrogenolysis of ester groups.

1. Introduction

Dimethyl 1,4-cyclohexane-dicarboxylate (DMCD) is widely applied in the manufacture of coating resin, polyester resin, alkyd resin, and plasticizers.[1–3] In industry, DMCD is produced by hydrogenation of DMT using palladium-based heterogeneous catalysts at temperatures ranging from 160 to 180 °C under a high pressure of H_2.[4] Given the harsh conditions and the use of the noble metal palladium, it is urgent to develop a mild and inexpensive catalytic reaction protocol.

In the last decades, various Pd, Ru, or Ni catalysts were developed for DMT hydrogenation to DMCD. Zhang *et al.* reported a supported $Pd/HT_C\text{-}Al_2O_3$ catalyst giving excellent conversion and selectivity.[5] Tan *et al.* prepared supported Ru_5/Al_x SBA-15 with 100% selectivity and 93.4% yield (100 °C, 4.14 MPa H_2).[6] As a non-noble metal case, $Ni/Ni(Al)O_x/AlO_x$ catalysts were successfully used with a selectivity of 93.3% and almost complete conversion of DMT.[7] A modified skeletal Ni catalyst was produced, yielding DMCD with complete conversion and 92.0% selectivity.[8] Despite high selectivity to DMCD, small amounts of byproducts (Scheme 1) were commonly generated with nickel catalysts, whereas almost stoichiometric selectivity could be achieved by using noble metal catalysts.

Various strategies have been employed to enhance activity and selectivity, such as utilizing supported bimetallic Ru–Ni/CNT catalysts[9] or Re-modified Ru-based catalysts.[10] While most studies focus on noble metal catalysts, investigations into modified nickel catalysts for improving catalytic activity and product selectivity are rare. The main by-products of nickel catalysts are due to the hydrogenolysis of the ester group (Scheme 1, products 5 and 6). For example, aryl esters can be activated into tolyl derivatives by homogeneous Ni catalysts, followed by hydrogenolysis using Ni/NHC catalysts.[11] Multifunctional $Pt/WO_3\text{–}ZrO_2$ catalysts promote hydrogenolysis with excellent alkanes selectivity, where the acidity of support is critical.[12] Therefore, using an appropriate alkaline promoter might be helpful to inhibit the hydrogenolysis of ester.

In this study, potassium-modified nickel catalysts were prepared using the AE method (ammonia evaporation) and applied to the selective hydrogenation of DMT. H_2-TPR results

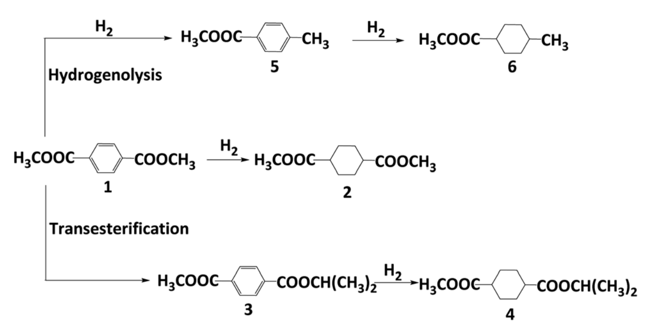

Scheme 1 Reaction network of DMT hydrogenation on Ni-based catalysts.

[a]School of Chemical Engineering, Guizhou Minzu University, Guiyang 550025, P. R. China

[b]State Key Laboratory for Oxo Synthesis and Selective Oxidation, Lanzhou Institute of Chemical Physics (LICP), Chinese Academy of Sciences, Lanzhou 730000, P. R. China. E-mail: yhli@licp.cas.cn

[c]College of Chemistry and Molecular Engineering, Qingdao University of Science and Technology, Qingdao 266000, P. R. China

† Electronic supplementary information (ESI) available: Catalyst characterization, evaluation of the catalytic performance, Fig. S1–S3, and Tables S1–S3. See DOI: https://doi.org/10.1039/d3ra02223d

‡ These two authors contributed equally.

indicate a significant decrease in reduction temperature for K-modified catalysts, which indicates that more metallic nickel species exist compared to pristine Ni/SiO_2 under the same conditions. NH_3-Temperature Programmed Desorption (NH_3-TPD) results show moderate strength acid sites vanished on potassium-modified Ni/SiO_2 catalysts, which is likely due to neutralization between K_2O and acid sites. Catalysts modified with K-promoter exhibit higher activity and selectivity than pristine Ni/SiO_2. Among K-modified catalysts, KF-Ni/SiO_2 catalyst is the best catalyst regarding conversion and selectivity (95% conversion and 96% selectivity). The high DMCD selectivity of K-modified catalysts is attributed to lower reduction temperature and smaller acid sites which inhibit hydrogenolysis of ester to alkane.

2. Experimental

2.1 Preparation of catalysts

Synthesis of Ni/SiO_2 catalyst. The AE method was used to synthesize Ni/SiO_2 catalyst with a preset nickel loading of 20 wt%.[13] As a typical procedure: in 180 mL of deionized (DI) water, 20 g of ethylene glycol was added. 5.0 g $Ni(NO_3)_2 \cdot 3H_2O$ (A. R. Hushi) was added to the ethylene glycol solution above. 75 mL of 5 wt% ammonia solution (A. R. Hushi) was added and stirred for 20 min to form a blue solution (pH ≈ 11–12). Subsequently, 16.7 g of colloidal silica (30 wt%, Qingdao Bay Chemical Co., LTD, China) was added and stirred for 4 hours. Ammonia was evaporated by stirring the solution at 80 °C for 5–6 h until pH was 6–7. The obtained solids were separated by filtration, washing, and overnight drying (80 °C). The powder obtained was designated as Ni/SiO_2 drying precursor.

Synthesis of K-modified Ni/SiO_2 catalyst. The impregnation method was employed to generate K-modified catalysts. Briefly, in 1 mL of DI water, desired amount of potassium salts (KVO_3, A. R. Aladdin; KOH, A. R. Aladdin; KF, A. R. Aladdin) with a preset potassium loading of 0.5 wt% was dissolved to acquire a solution of potassium salt. The solution was added dropwise to Ni/SiO_2 drying precursor until the surface was completely covered. The precursors were aged for 3 h at room temperature and dried overnight at 80 °C.

All catalyst precursors were calcinated at 450 °C for 4 h under ambient conditions. The samples were then reduced in pure H_2 flow (30 mL min^{-1}) for 4 h at a certain temperature (400 °C, 500 °C, 550 °C) with a heating rate of 3 °C min. M-Ni/SiO_2 catalysts were obtained, where *M* is the promoter (KVO_3, KOH, KF).

3. Results and discussion

3.1 Structural characterization of catalysts

H_2-TPR characterization was first carried out to determine the influence of promoters on the reducibility of nickel species on SiO_2 support. For the pristine Ni/SiO_2 sample (Fig. 1(a)), a broad reduction peak ranging from 400 to 700 °C is assigned to the reduction of nickel silicate hydrate to Ni^0. The peak center at approximately 590 °C is much higher than Ni/SiO_2 produced by sol–gel[14] or wet impregnation (WI).[15] The higher reduction temperature indicates that the AE method can enhance the metal–support interaction.[16,17]

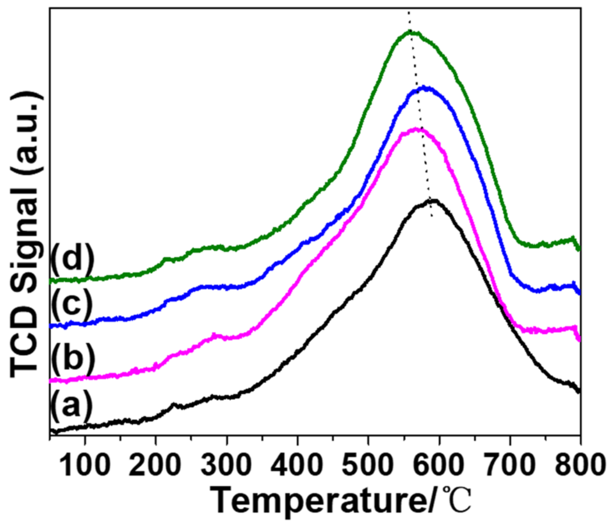

Fig. 1 H_2-TPR profiles of catalysts and promoters are in the following sequence: none (a); KVO_3 (b); KOH (c); KF (d).

As a typical alkali metal hydrogenation dopant, potassium typically hinders catalyst reduction by inhibiting the adsorption and dissociation of hydrogen.[18] Chen has reported that K_2O inhibits reduction of Ni^{2+} in Ni/SiO_2 catalysts.[19] However, in our catalytic system, the reduction temperatures of K-modified catalysts are lower than that of Ni/SiO_2. It is reported that the introduction of Mo element can weaken the interaction between Ni^{2+} species and phyllosilicates.[20] Therefore, the introduction of alkaline dopants might weaken interactions between Ni and phyllosilicates, resulting in a reduction temperature higher than nickel oxide but lower than nickel phyllosilicates. On the other hand, the promoting effect of V_2O_5 and F can facilitate the reduction of nickel phyllosilicate.[21,22] The sequence of reduction temperatures is shown as follows: (a) > (c) > (b) > (d). Besides, the reducibility of each catalyst was calculated and listed in Table S1.†

H_2-TPD was performed to investigate the effects of potassium on the adsorption properties of hydrogen on metallic Ni (Fig. S1†). All catalysts showed two peaks, the peak at a lower temperature can be attributed to hydrogen chemisorption on metallic Ni. The H_2 desorption peak at high temperatures can likely be attributed to the hydrogen chemisorbed on the Ni of nickel phyllosilicates. The dispersion of nickel is calculated and listed in Table S1.†

Fig. 2 depicts X-ray diffraction (XRD) patterns of M-Ni/SiO_2 (M = KVO_3; KOH; KF) samples following calcination and reduction. For all calcined samples (Fig. 2A), characteristic peaks at $2\theta = 34.6°$ and 60.6° are assigned to (110) and (300) facets of nickel silicate hydrate (JCPDS 20-0790), respectively, which is consistent with previous reports.[23] Amorphous SiO_2 is responsible for the wide peak centered at $2\theta = 22.2°$ (JCPDS 76-0933).[24] No characteristic peak corresponding to NiO indicates that nickel species are primarily nickel phyllosilicates. Although the broad reduction peak starts from 400 °C according to H_2-TPR results, no obvious new characteristic peaks can be observed after reduction at 400 °C for 4 hours (Fig. S2†).

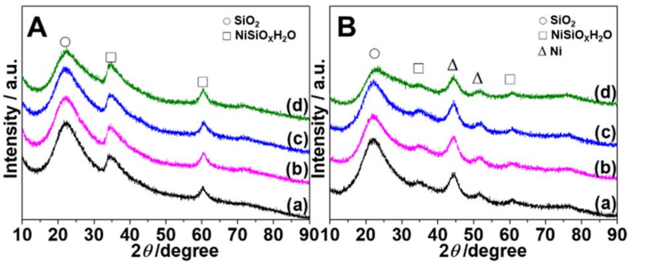

Fig. 2 XRD patterns of (A) calcined (450 °C/4 h) and (B) reduced (550 °C/4 h) catalysts. From bottom to top, promoters are in the following sequence: none (a); KVO_3 (b); KOH (c); KF (d).

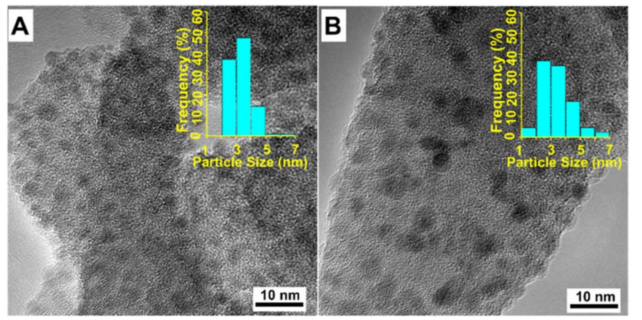

Fig. 3 TEM images of Ni/SiO_2 (A), and KF-Ni/SiO_2 (B).

Increasing the reduction temperature to 500 °C (Fig. S3†), two new peaks at $2\theta = 44.5°$ and $51.8°$ ascribed to (111) and (200) of Ni^0 (JCPDS 04-0850) can be observed.[9] Nickel silicate hydrate remains the main species at this temperature. Increasing the reduction temperature to 550 °C, the intensity of the two new peaks increases (Fig. 2B). Although the majority of nickel silicate species are reduced to metallic nickel, some nickel phyllosilicate species ($2\theta = 34.6°$ and $60.5°$) still exist even after 4 h of reduction in pure H_2 at 550 °C. Among the four catalysts, KF-Ni/SiO_2 has the weakest peak intensity of nickel silicate species. The crystallite size of the Ni^0 nanoparticle is determined using the FWHM of Ni^0(111) based on the Scherrer equation (Table 1). The results demonstrate that adding potassium promoter did not alter the peak intensity of nickel particles or appreciably alter their size.

The chemical compositions and textural properties of catalysts were listed in Table 1. Nickel ions weakly adsorbed on silica gel were easy to elute during the centrifugal washing process, therefore, the actual nickel loading was slightly lower than the preset value (about 14 wt% *vs.* 20 wt%). The loading of K is close to the preset values (about 0.4 wt% *vs.* 0.5 wt%) determined by ICP-MS. BET surface area (S_{BET}), pore volume (V_p), and average pore size (D_p) of catalysts were measured using N_2 adsorption–desorption isotherms (Table 1). Both pristine Ni/SiO_2 and KOH-modified catalysts exhibit large S_{BET}, Vp, and D_p. Adding potassium promoters significantly affects the physical properties of catalysts. A drop in S_{BET} and V_p indicates that K species have occupied pore channels of support, which is consistent with previous reports.[18] KF-Ni/SiO_2 catalyst possesses the smallest surface area, volume, and pore size. Except for the fact that K^+ occupies part of pore channels, the reaction between F ion and SiO_2 can also cause the collapse of the pore structure. This is consistent with the H_2-TPR and XRD results, where the weakening of interaction results in lower reduction temperature and fewer amounts of nickel phyllosilicates.

Transmission electron microscopy (TEM) was used to investigate the dispersion and shape of reduced catalysts (Fig. 3). For the Ni/SiO_2 catalyst, most of particle sizes range from 2 to 5 nm (Fig. 3A), suggesting an excellent dispersity of Ni nanoparticles on SiO_2 support. As magnetic catalysts may cause damage to TEM measurement, KF-Ni/SiO_2 sample was chosen to illustrate the influence of potassium promoters on Ni dispersion(Fig. 3B). Compared with Ni/SiO_2 catalyst, particle size distribution becomes wider. Even though most particle sizes range from 2 to 5 nm, there are more small (1 to 2 nm) and large (5 to 7 nm) particles in KF-Ni/SiO_2. The etching of SiO_2 by fluoride ions may lead to the collapse of pore structure, leading to small or large nickel particles. Nevertheless, the average particle sizes of the two catalysts are similar, which is in accordance with previous reports.[20] Combined with TEM and XRD results, it can be considered that introducing small amounts of K did not significantly change the size of nickel particles.

The surface acidity of potassium-promoted Ni/SiO_2 catalysts was evaluated using NH_3-Temperature Programmed Desorption (NH_3-TPD) (Fig. 4). All catalysts showed a desorption peak attributed to weak acid sites at around 100 °C, which was caused by NH_3 adsorption on weak acidic support SiO_2. In addition, a broad desorption peak in temperatures ranging from 250 to 350 °C, assigned to moderate-strength acid sites, can be observed (Fig. 4(a)). The nickel phyllosilicate surface or edge of

Table 1 Structural properties and chemical compositions of M-Ni/SiO_2 catalysts

Catalysts (M-Ni/SiO_2)[a]	Loading[b] (wt%) Ni	K	Crystallite size[c] $(nm)^{-1}$	S_{BET}[d] ($m^2\ g^{-1}$)	V_p[e]e ($cm^3\ g^{-1}$)	D_p[f] (nm)
Ni/SiO_2	13.7	—	3.4	329	0.70	8.5
KVO_3-Ni/SiO_2	14.9	0.45	3.0	307	0.62	8.0
KOH-Ni/SiO_2	13.0	0.44	3.3	314	0.73	9.3
KF-Ni/SiO_2	13.8	0.38	3.0	261	0.64	8.5

[a] M stands for potassium dopant. [b] Loadings of Ni and K are determined by ICP-MS. [c] Calculated by using the Ni (111) reflection at 44.5° based on the Scherrer equation, catalyst was reduced at 550 °C. [d] BET specific surface area. [e] Total pore volume. [f] BJH desorption average pore diameter.

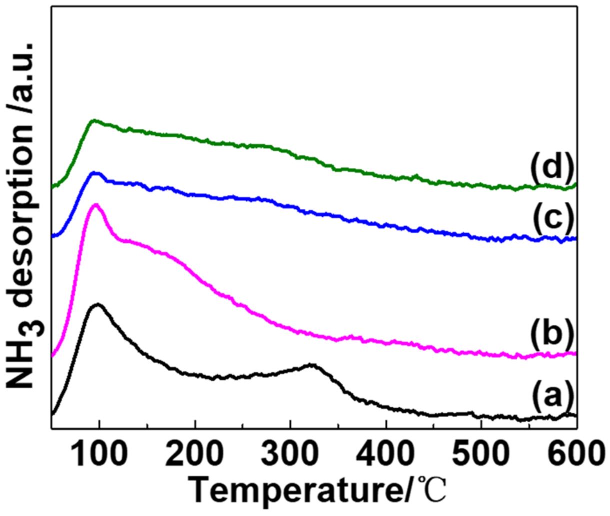

Fig. 4 NH_3-TPD profiles of catalysts and promoters are in the following sequence: none (a); KVO_3 (b); KOH (c); KF (d).

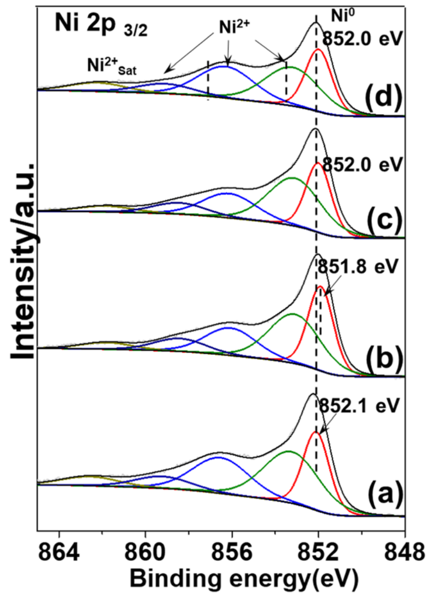

Fig. 5 XPS spectra of the reduced catalysts and promoters are in the following sequence: none (a); KVO_3 (b); KOH (c); KF (d).

Ni(II) is a primary source of acid sites for AE-prepared pristine Ni/SiO_2 catalysts.[17,20,25]

NH_3 desorption peaks of K-modified catalysts exhibit significant differences. For KVO_3 modified catalyst (Fig. 4(b)), the moderate-strength acid desorption peak vanished, and a shoulder peak ascribed to a weak acid desorption peak, being centered at 150 to 250 °C, was observed. This is due to the combined contribution of K_2O and V_2O_5 oxides, which is formed by calcination of KVO_3 in the air. K_2O neutralizes moderate-strength acid sites, which is resulted from –OH group in phyllosilicates, and V_2O_5 produces a new weak acid site desorption peak. For KOH and KF-modified catalysts (Fig. 4(c) and (d)), the desorption peak assigned to the moderate-strength peak vanished, and the desorption peak intensity of weak acid sites decreased. These results indicate that only a 0.5 wt% addition of alkaline potassium dopants can significantly decrease the acidity of catalysts. Although the peak intensity decreased to some extent, the desorption temperature of NH_3 on weak acid sites was almost the same among the four catalysts. These results are consistent with previous reports,[26,27] where alkali salt could decrease the acidity of Ni/SiO_2 catalysts by neutralizing acid sites but did not change the strength distribution of acidity.

The electronic structural information of potassium-modified catalysts was probed using X-ray photoelectron spectra (XPS). According to previous reports, two typical nickel species co-exist in nickel phyllosilicate (1 : 1 Ni–PSi, formula: $Si_2Ni_3O_5(OH)_4$ and 2 : 1 Ni–PSi, formula: $Si_4Ni_3O_{10}(OH)_2$).[13,28] For pristine Ni/SiO_2 catalyst (Fig. 5(a)), the spectra were deconvoluted into five peaks centered at around 852.1 eV, 853.3 eV, 856.5 eV, 859.2 eV, and 862.5 eV corresponding to Ni^0, Ni^{2+} of nickel oxide, 1 : 1 Ni–PSi, 2 : 1 Ni–Psi, and Ni^{2+} satellite peak, respectively. For KVO_3-Ni/SiO_2 catalyst (Fig. 5(b)), a slight shift of 0.2 eV was observed on Ni^0 $2p_{3/2}$ peak. This is due to vanadium species increasing the electron charge density of Ni atoms, consistent with previous reports where V_2O_5 can effectively improve the dispersion of nickel in Ni/FDU-12 catalyst and alter the electron charge density of nickel.[29]

Adding KOH or KF to a pristine Ni/SiO_2 catalyst had little effect on the chemical valence state of Ni^0 (from 852.1 eV to 852.0 eV) (Fig. 5(c) and (d)). Besides Ni^0 species, Ni^{2+} species attributed to nickel oxide and nickel phyllosilicates species were also observed. This is consistent with XRD results where there were characteristic peaks attributed to nickel phyllosilicates species. The multiple Ni species can also explain the broad reduction peak in H_2-TPR results. The deconvoluted area and fraction of different Ni species are listed in Table S2.†

Evaluation and optimization of catalysts. The performance of Ni catalysts is closely linked to the amount of metallic nickel present.[30] To investigate this relationship, catalytic performances of catalysts reduced at different temperatures were tested for DMT hydrogenation to DMCD. Primarily, the calcined samples were applied to DMT hydrogenation to investigate the catalytic activity of Ni^{2+} and the results are shown in Table S3.† From Table S3† we can see that the calcined samples showed no catalytic activity and DMCD selectivity. Catalysts reduced at 400 °C showed poor performances with a conversion of less than 30% and selectivity of less than 80% (Fig. 6A). Combined with XRD results (Fig. S2†), it was found that catalysts were not well reduced to Ni^0, despite the presence of promoters to facilitate the reduction process. The main byproduct (detailed selectivities are given in Table S3†) observed was 1-methyl 4-(1-methyl ethyl) ester (Scheme 1, product 3), resulting from a transesterification reaction between DMT and solvent isopropanol. As transesterification and hydrogenation reactions are competitive, a lower amount of metallic nickel in catalysts led to lower hydrogenation activity, and consequently, the increase of transesterification products. To enhance the

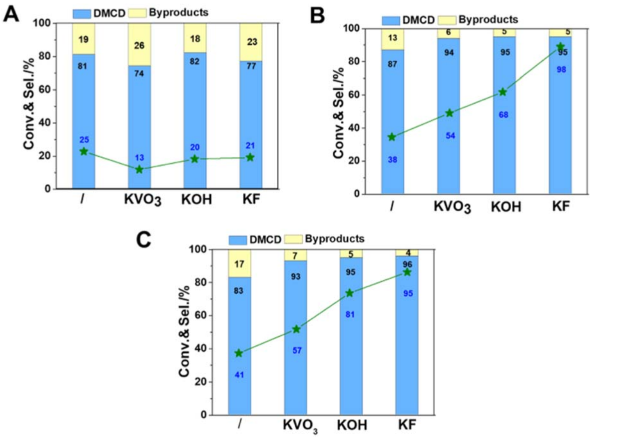

Fig. 6 Influence of reduction temperature of catalysts. 400 °C (A); 500 °C (B); 550 °C (C). Reaction conditions: catalyst, 50 mg; DMT, 0.1 g; IPA, 2 mL; the initial pressure of H_2, 5 MPa; reaction temperature, 90 °C; reaction time, 4 h.

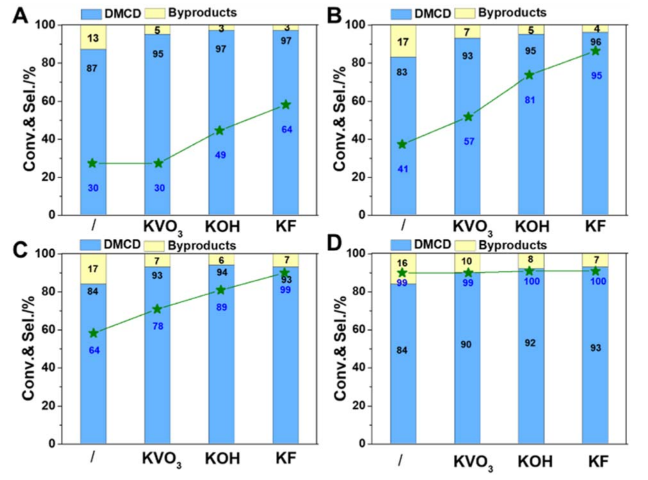

Fig. 7 Influence of reaction temperature. 80 °C (A); 90 °C (B); 100 °C (C); 110 °C (D). Reaction conditions: catalyst, 50 mg; DMT, 0.1 g; IPA, 2 mL; the initial pressure of H_2, 5 MPa; reaction time, 4 h.

selectivity of DMCD, it is essential to increase the reduction temperature to increase the amount of metallic nickel. The elevated reduction temperature (500 °C) improved both conversion and selectivity significantly (Fig. 6B). Additionally, catalysts with dopants showed higher conversion and DMCD selectivity compared to Ni/SiO_2, with conversion and selectivity in order of KF > KOH > KVO_3. The significant improvement in performance is attributed to the increased proportion of nickel silicate hydrate species to metallic nickel. Further increasing reduction temperature to 550 °C did not show any clear difference in conversion and selectivity(Fig. 6C). The stable catalytic activity indicates that catalysts are not sintered even if reduced at 550 °C.

Considering catalysts reduced at 550 °C have more metallic nickel, they have been chosen as model catalysts to explore the effect of reaction temperature. All catalysts displayed catalytic activity even at a low temperature of 80 °C. Potassium promoters were found to greatly enhance the selectivity of DMCD, with KF-Ni/SiO_2 achieving a remarkable 97% selectivity (Fig. 7A). Nickel-based catalysts can catalyze efficiently the hydrogenolysis of the fatty acid ester, and excellent hydrodeoxygenation performance of methyl palmitate to alkanes was acquired due to the abundant acidic sites in modified nickel phyllosilicate catalysts.[20] In this work, the introduction of promoters had two key effects: it effectively lowered reduction temperature, thus increasing the proportion of metallic nickel in modified catalysts compared to Ni/SiO_2, and neutralized moderate strength acid sites, decreasing hydrogenolysis of ester to alkanes.[12] This represents the highest selectivity catalyzed by a non-precious metal catalyst. The conversion of DMT increased as the reaction temperature increased from 80 to 100 °C (Fig. 7B and C), whereas the selectivity of DMCD remained substantially constant. Further increasing the reaction temperature to 110 °C, all catalysts achieved 100% DMT conversion. The main byproduct, methyl 4-methyl-cyclohexane carboxylate (MMCHC) (Scheme 1, product 6), is resulted from the hydrogenation of methyl 4-Methylbenzoate (MMB) (Scheme 1, product 5). Detailed selectivities of the main byproducts are given in Table S4.†

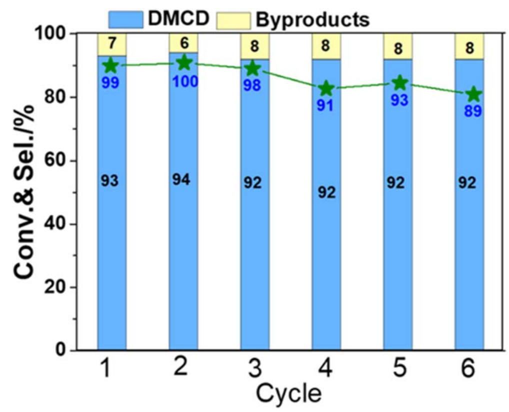

Fig. 8 Stability studies for KF-Ni/SiO_2 catalyst on DMT conversion and DMCD selectivity. Reaction conditions: catalyst, 50 mg; DMT, 0.1 g; IPA, 2 mL; the initial pressure of H_2, 5 MPa; reaction temperature, 100 °C, reaction time, 4 h.

The stability of catalysts is an important consideration when assessing their possible usage in industry. To test the stability of KF-Ni/SiO_2, which is an optimal catalyst, it underwent a six-time recycling test (Fig. 8). The catalyst was filtered, washed three times with isopropanol, and directly reused in the next cycle without additional processing or reduction. The DMT conversion was above 98% until the third cycle. After the sixth cycle, it decreased to 89%. The selectivity of DMCD remained consistent throughout six cycles, indicating that the catalyst did not lose its activity or selectivity over time. These results demonstrate that the catalyst exhibited good stability over the course of the recycling test.

4. Conclusions

In summary, this study developed a potassium-promoted strategy to enhance the selectivity of DMCD during the hydrogenation of DMT. Catalytic performance evaluation showed both conversion and selectivity were significantly improved on K-modified catalysts compared to pristine Ni/SiO_2. KF-promoted Ni/SiO_2 showed the highest conversion and selectivity within the evaluated range. The remarkable difference in activity and selectivity is due to the lower reduction temperature, which can offer higher amounts of metallic nickel under the same conditions, as well as smaller amounts of acid sites inhibiting the hydrogenolysis of ester. Additionally, the selectivity and reactivity of the KF-promoted catalyst remained consistent throughout six recycling experiments, demonstrating its excellent stability. Overall, the present work provides comprehensive insights into the rational design of nickel catalysts by using potassium modifiers.

Additional reference cited within the ESI.†[31]

Author contributions

Han Xiao: investigation, formal analysis, validation, data curation, writing – original draft. Chao Zhang: investigation, formal analysis, data curation. Jiaojiao Zhao: formal analysis, visualization, writing – review & editing. Zhaohui Zheng: formal analysis, software. Yuehui Li: conceptualization, supervision, resources, funding acquisition.

Conflicts of interest

The authors declare no competing financial interest.

Acknowledgements

The authors are grateful for the financial support from NSFC (21633013, 22102197), funding support from Jiangsu Province Natural Science Foundation (BK20211096), and Guizhou Provincial Science and Technology Projects (ZK[2021]051). Dr Zhao thanks the Science Fund of Shandong Laboratory of Advanced Materials and Green Manufacturing (Yantai, AMGM2021F07).

Notes and references

1 S. R. Turner, *J. Polym. Sci., Part A: Polym. Chem.*, 2004, **42**, 5847.
2 B. J. Sublett and G. W. Connell, *US Pat.* 5559159, 1996.
3 R. R. Ambrose, J. B. O'dwyer, B. K. Johnston, D. P. Zielinski, S. Porter and W. H. Tyger, *US Pat.* 4859743, 1989.
4 D. Hou, J. Xin, X. Lu, X. Guo, H. Dong, B. Ren and S. Zhang, *RSC Adv.*, 2016, **6**, 48737.
5 F. Zhang, J. Chen, P. Chen, Z. Sun and S. Xu, *AIChE J.*, 2012, **58**, 1853.
6 W. Yu, S. Bhattacharjee, W.-Y. Lu and C.-S. Tan, *ACS Sustainable Chem. Eng.*, 2020, **8**, 4058.
7 Q. Fan, X. Li, Z. Yang, J. Han, S. Xu and F. Zhang, *Chem. Mater.*, 2016, **28**, 6296.
8 X. Xu, Z. Rong, W. Du, F. Zheng, Y. Liang, Y. Wang and L. Lv, *Fine Chem.*, 2010, **27**, 1239.
9 Y. Huang, Y. Ma, Y. Cheng, L. Wang and X. Li, *Ind. Eng. Chem. Res.*, 2014, **53**, 4604.
10 E. Qu, J. Luo, X. Di, C. Li and C. Liang, *J. Nanosci. Nanotechnol.*, 2020, **20**, 1140.
11 A. Cook, S. Prakash, Y.-L. Zheng and S. G. Newman, *J. Am. Chem. Soc.*, 2020, **142**, 8109.
12 K. Yuan, Y. Yamazaki, X. Jin and K. Nozaki, *J. Am. Chem. Soc.*, 2023, **145**, 3454.
13 Y. Wu, G. Chang, Y. Zhao and Y. Zhang, *Dalton Trans.*, 2014, **43**, 779.
14 F. Ding, Y. Zhang, G. Yuan, K. Wang, I. Dragutan, V. Dragutan, Y. Cui and J. Wu, *J. Nanomater.*, 2015, **16**, 60.
15 T. A. Le, J. K. Kang and E. D. Park, *Top. Catal.*, 2018, **61**, 1537.
16 P. Burattin, M. Che and C. Louis, *J. Phys. Chem. B*, 2000, **104**, 10482.
17 Y. W. Wang, Y. J. Zhang, K. J. Wang, L. M. Tan and S. Y. CHEN, *J. Fuel Chem. Technol.*, 2021, **49**, 97.
18 Y. Yang, H.-W. Xiang, Y.-Y. Xu, L. Bai and Y.-W. Li, *Appl. Catal., A*, 2004, **266**, 181.
19 J. Chen, J. Zhang and J. Zhang, *React. Kinet. Catal. Lett.*, 2008, **93**, 359.
20 (*a*) B. Peng, Y. Yao, C. Zhao and J. A. Lercher, *Angew. Chem., Int. Ed.*, 2012, **51**, 2072; (*b*) B. Peng, X. Yuan, C. Zhao and J. A. Lercher, *J. Am. Chem. Soc.*, 2012, **134**, 9400; (*c*) L. Yan, X. X. Liu, J. Deng and Y. Fu, *Green Chem.*, 2017, **19**, 4600.
21 Y. Zhang, Y. Chen and Q. Liu, *Int. J. Hydrogen Energy*, 2021, **46**, 32003.
22 M. Ebrahiminejad and R. Karimzadeh, *Mol. Catal.*, 2022, **517**, 112056.
23 S. Yuan and L. Zhao, *RSC Adv.*, 2016, **6**, 49769.
24 K. Xu, J.-X. Wang, X.-L. Kang and J.-F. Chen, *Mater. Lett.*, 2009, **63**, 31.
25 F. Dong, G. Ding, H. Zheng, X. Xiang, L. Chen, Y. Zhu and Y. Li, *Catal. Sci. Technol.*, 2016, **6**, 767.
26 J. Chang, N. Tsubaki and K. Fujimoto, *J. Jpn. Pet. Inst.*, 2000, **43**, 357.
27 S. Xie, H. Li, H. Li and J.-F. Deng, *Appl. Catal., A*, 1999, **189**, 45.
28 Z. Li, L. Mo, Y. Kathiraser and S. Kawi, *ACS Catal.*, 2014, **4**, 1526.
29 Z. Tian, H. Yang and Q. Liu, *Energy Technol.*, 2020, **8**, 1901270.
30 S. Abelló, D. Verboekend, B. Bridier and J. Pérez-Ramírez, *J. Catal.*, 2008, **259**, 85.
31 F. Wang, C.-M. Li, X.-Y. Zhang, M. Wei, D. G. Evans and X. Duan, *J. Catal.*, 2015, **329**, 177.